

APPLICATION OF THIRD-ORDER TRANSFER FUNCTIONS FOR EDGE ENHANCEMENT OF SIGNALS FROM SCANNED IMAGING SYSTEMS¹

RADAMES K. H. GEBEL AND HENRY E. FETTIS

*Aerospace Research Laboratories, LS, Wright-Patterson AFB, Ohio 45433, and
The Ohio State University; and Aerospace Research Laboratories, LB,
Wright-Patterson AFB, Ohio 45433*

ABSTRACT

Whenever images are reproduced by the utilization of a time-sequential signal obtained by electron beam scanning or by flying-spot light-scanning of photo-conductive thin-films, etc., onto which an optical image is focused, lack of edge resolution occurs. This is due to a number of intrinsic, uncontrollable factors of the semiconductor, e.g., its finite thickness, finite size of the scanning beam, etc. Such lack of edge resolution makes difficult the determination of the exact configurations of imaged objects. The present paper describes a linear network composed of an operational amplifier arrangement which allows controllable steepening (crispening) of edge resolution even when the peaks of the edges are overemphasized. This is accomplished without causing the post-transient oscillations which conventional devices tend to introduce. The mathematical relationships of the electronic crispening set-up are derived, and transfer functions in the Laplace-frequency-, and time domains are analyzed. The Nyquist diagram of a typical arrangement shows that the system is stable even when it produces, from a unit step input, an output signal with an overshoot of 250%. Further the resulting signal is free of oscillations, in contrast to the second order system which exhibits permanent oscillations when producing an overshoot of only 100%. The phase and amplitude behavior for the second and third order system are compared. It is shown that the phase of the second order system is an increasing function of frequency with a steep slope at the critical value whereas the third order system exhibits a gradually increasing and then decreasing phase. Further, the amplitude response of the second order system rises sharply as resonance is approached, while for the third order system there is a gradual peaking of the amplitude characteristic. The smoothing effect of the system on a signal exhibiting white noise is demonstrated; the out-put signal being virtually free of any noise components.

PREFACE

Recently the senior author analyzed experimentally obtained physiological data of the muscle and the muscle-spindle characteristics (muscle data: Creed *et al.*, 1930; spindle data: Lippold *et al.*, 1960), from a bio-electrical viewpoint (topics suggested by Prof. Dr. Herman R. Weed, The Ohio State University). His interest was especially captured by the particular unit step-response of the spindle receptor, and since the spindle unit step-response cannot be produced by an ordinary underdamped second-order system it was surmised that the spindle receptor might essentially act analogously to a closed-loop feedback arrangement controlled by the central nervous system and having a time constant in the feedback loop which is larger by a significant factor than that of the forward loop. In accordance with the above ideas, an electrical passive-analog set-up for the spindle receptor was designed and the required pertinent time constants determined from the physiological data whereby the set-up behaves (within tolerance) as an organic-spindle receptor-system. The transfer function of this passive-analog spindle-circuit was then determined in the Laplace and in the time domains in order to synthesize the spindle response, using an appropriate arrangement of operational amplifiers. In the same manner, using the physiological muscle data, an electronic-passive-analog muscle arrangement was designed and its transfer function determined. Having derived from biological data a valid transfer

¹Manuscript received August 16, 1971.

function for the spindle-response as well as for the muscle characteristic, both transfer functions were represented by a closed-loop-analog-computer arrangement for the purpose of studying the joint characteristics of the muscle and spindle-receptor behavior. From the appearance of the step response data obtained with the above set-up, Gebel intuitively conceived the idea that, if the spindle function used in the feedback loop were to be employed as forward function, and the muscle function used in the forward section were to be employed in the feedback loop, the combination would yield a third-order function which could be called a reversed muscle and spindle function, and which would achieve edge steepening in edge-deteriorated images without the occurrence of post-transient oscillations. Tests performed later proved the correctness of this idea. The closed-loop muscle-and-spindle system was then transformed into a collapsed single-transfer function in the Laplace domain. The derivation of the corresponding transfer function in the time domain, including the effect of time delay, proved to be a very difficult task however, which was successfully solved in explicit form by the co-author, employing contour integration in the complex ω -plane as well as the s -plane.

INTRODUCTION

Lack of edge resolution may show up in images which are reproduced by the utilization of a time-sequential signal obtained by electron-beam scanning or by flying-spot light-scanning of photoconductive thin-films, etc., onto which an optical image is focused. This lack of edge resolution may be due to finite thickness of the film, finite size of the scanning beam, unfavorable lateral-to-transverse ratio of the involved effective resolution-element size, an insufficient bandwidth in the transmission path, etc. The lack of edge resolution may make difficult the determination of the dimensions and exact configuration of imaged objects. Attempts to restore the sharpness of the edges by employing a network with appropriate peaking coils, etc., *i.e.* by the use of an ordinary under-damped second-order system, may improve the sharpness of the edges, but very annoying post-transient oscillations are usually introduced into the signal in an attempt to force sufficient steepness of the edges. Second-order systems have been extensively treated (Jacobson and Ayre, 1958) and summarized in graphical form (Ayre, 1961). An inspection of the results presented there shows that no conventional underdamped second-order system can produce an overshoot of greater than 100 percent, and the achievement of even a significant fraction of this is unrealizable in practice, as will be shown later. If post-transient oscillations are to be kept within two percent of the steady-state value, then in the case of a unit-step input, the gained overshoot is less than two percent. It is thus evident that an ordinary second-order system will not be suitable for any significant edge sharpening, since the purpose here is to produce overshoot in signals which have deteriorated, *i.e.*,

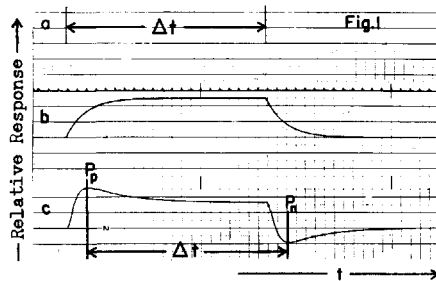


FIGURE 1. Time sequential signal showing unit step function as consecutively modified by first- and third-order systems.

in ones where the original unit-step inputs have been modified by a first-order system, and which are therefore changing in a gradual fashion, rather than as a step function.

Several time-sequential signals are shown in figure 1, each representing a single horizontal line. The first (1a), which consists of a positive and a negative unit-step, depicts the information one would get under ideal conditions, when optically scanning a black bar against a bright background, or vice versa. Figure 1b shows the deterioration of the same signal by a first-order system, such as occurs, for example, in the transmission of a signal over a long uncorrected cable, or over any other first-order system having an insufficient bandwidth. If the signal in figure 1b were to be used for the modulation of the electron beam of a cathode ray tube, the reproduced image would, instead of changing fairly suddenly from black to white (or vice versa), show a very gradual change, which is usually referred to in "shop language" as a "smeary picture".

SIGNAL MODIFICATION BY A THIRD-ORDER SYSTEM

Let the signal show in figure 1b be further modified by a third-order network having a transfer function (reversed-muscle-and-spindle function) represented in the Laplace domain by

$$(1) \quad F_R(s) = \frac{e_o}{e_i} = \frac{(1+s\tau_1)}{1+K_F \frac{(1+s\tau_2)(1+s\tau_3)}{(1+s\tau_1)}},$$

where s is the Laplace variable in sec^{-1} , τ_1 , τ_2 , τ_3 , and γ are time constants in sec ; and K_F is an attenuation factor. Then, if the involved values are properly chosen, a signal as shown by figure 1c will result. The signal shown in figure 1c is not congruent with the ideal signal of figure 1a, which constitutes the intensity distribution of one line of the optical image. However, an image produced by a signal of figure 1c appears on a cathode ray tube, or other recording media, as free of "smear" and gives a crisp representation of the edges of the imaged objects. Visual interpretation of object boundaries in the image will be based on observing the positive and negative peaks marked with P_p and P_n . Comparison of the signal in figure 1c with that in figure 1a shows that the time base has shifted, but that the dimension of the object as represented by the time interval Δt between the positive and negative unit step of figure 1a has not changed. The significance of figure 1c is that no "ringing" (a "shop expression" for post-transient oscillation) has been introduced.

THE TRANSFER FUNCTION IN THE TIME DOMAIN

A third-order network with a transfer function in the Laplace domain as expressed by equation 1 has in the time domain a transfer function of the form

$$(2a) \quad h(t) = F[Ae^{-r_1 t} + Be^{-r_2 t} + Ce^{-r_3 t}] \quad [\text{sec}^{-1}],$$

where r_1 , r_2 , and r_3 in sec^{-1} are the roots of the third-order equation

$$(3a) \quad s^3 - \beta_1 s^2 + \beta_2 s - \beta_3 = 0 \quad [\text{sec}^{-3}].$$

The coefficients depend on the system parameters, i.e.

$$(4) \quad \beta_1 = \left(\frac{1}{\gamma} + \frac{1}{\tau_2} + \frac{1}{\tau_3} \right) \quad [\text{sec}^{-1}],$$

$$(5) \quad \beta_2 = \left(\frac{1}{\gamma\tau_2} + \frac{K_F\tau_1}{\gamma\tau_2\tau_3} + \frac{1}{\gamma\tau_3} + \frac{1}{\tau_2\tau_3} \right) \quad [\text{sec}^{-2}],$$

$$(6) \quad \beta_3 = \frac{1 + K_F}{\gamma\tau_2\tau_3} \quad [\text{sec}^{-3}],$$

$$(7) \quad F = \frac{\tau_1}{\tau_2\tau_3} \quad [\text{sec}^{-1}],$$

$$(8a) \quad A = \frac{r_1^2 - \alpha_1 r_1 + \alpha_2}{(r_2 - r_1)(r_3 - r_1)},$$

$$(9a) \quad B = \frac{r_2^2 - \alpha_1 r_2 + \alpha_2}{(r_1 - r_2)(r_3 - r_2)},$$

$$(10a) \quad C = \frac{r_3^2 - \alpha_1 r_3 + \alpha_2}{(r_1 - r_3)(r_2 - r_3)},$$

with

$$(11) \quad \alpha_1 = \frac{1}{\gamma} + \frac{1}{\tau_1} \quad [\text{sec}^{-1}],$$

and

$$(12) \quad \alpha_2 = \frac{1}{\gamma\tau_1} \quad [\text{sec}^{-2}].$$

If the system is excited by an arbitrary input function $f(t)$, rather than by a δ pulse, the resulting output $g_f(t)$ is given by the convolution integral

$$(13) \quad g_f(t) = \int_0^t h(t-t^*)f(t^*)dt^* \int_0^t h(t^*)f(t-t^*)dt^*,$$

where t^* is a dummy integration variable. For the case where $f(t)$ is a unit step $u(t)$, the above integral becomes

$$(14) \quad g_u(t) = \int_0^t h(t^*)dt^* = F \left[-\frac{A}{r_1}(1-e^{-r_1 t}) + \frac{B}{r_2}(1-e^{-r_2 t}) + \frac{C}{r_3}(1-e^{-r_3 t}) \right].$$

On the other hand, if the step input $u(t)$ is modified by a conventional first-order system with a time constant λ^{-1} [sec.], then the output $f_1(t)$ of the first-order system will be proportional to $e^{-\lambda t}$ and the resulting response of the third-order system to $f_1(t)$ will be given by

$$(15) \quad g_e(t) = Fe^{-\lambda t} \left[\frac{A}{r_1 - \lambda}(1-e^{-(r_1 - \lambda)t}) + \frac{B}{r_2 - \lambda}(1-e^{-(r_2 - \lambda)t}) + \frac{C}{r_3 - \lambda}(1-e^{-(r_3 - \lambda)t}) \right].$$

In the case where two of the roots of equation 3 either coincide or appear as complex conjugates, the above expressions must be modified. If equation 3a has a pair of complex roots, the denominator of the transfer function in the s domain can be factored into a linear and quadratic factor as follows:

$$(3b) \quad s^3 + \beta_1 s^2 + \beta_2 s + \beta_3 \equiv (s+r)(s^2 + 2ps + q)$$

and the transfer function in the time domain becomes

$$(2b) \quad h(t) = F \left[A e^{-rt} + e^{-pt} \left(B \cos \sqrt{q-p^2} t + \frac{c-pt}{\sqrt{q-p^2}} \sin \sqrt{q-p^2} t \right) \right]$$

where

$$(8b) \quad A = \frac{r^2 - \alpha_1 r + \alpha_2}{r^2 - 2pr + q},$$

$$(9b) \quad B = \frac{(\alpha_1 - 2p) + (q - \alpha_2)}{r^2 - 2pr + q},$$

and

$$(10b) \quad C = \frac{(\alpha_2 - q)r + (\alpha_1 q - 2p\alpha_2)}{r^2 - 2pr + q},$$

The equation 2b may be specialized for the case of a double root by taking $q = p^2$ and noting that

$$(3c) \quad \lim_{q \rightarrow p^2} \frac{\sin \sqrt{q-p^2} t}{\sqrt{q-p^2}} = t.$$

The result for this case is

$$(2c) \quad h(t) = F[Ae^{-rt} + e^{-pt}(B + [C - pB]t)].$$

The functions defined by equations 1 and 2 correspond in the frequency domain to the following expression

$$(16) \quad H(\omega) = \left\{ \frac{\frac{\Omega_1^2}{\Omega_2^2 \Omega_3^2}}{1 + K_F \frac{\Omega_1^2}{\Omega_2^2 \Omega_3^2 \Omega_4^2} + Z} \right\}^{1/2},$$

where

$$(17) \quad \Omega_1^2 = (1 + \omega^2 \tau_1^2),$$

$$(18) \quad \Omega_2^2 = (1 + \omega^2 \tau_2^2),$$

$$(19) \quad \Omega_3^2 = (1 + \omega^2 \tau_3^2),$$

$$(20) \quad \Omega_4^2 = (1 + \omega^2 \gamma^2),$$

$$(21) \quad Z = 2K_F \frac{\Omega_1}{\Omega_2 \Omega_3 \Omega_4} \cos \theta,$$

$$(22) \quad \Theta = \Theta_1 - \Theta_2 - \Theta_3 - \Theta_4 \quad [\text{radians}],$$

$$(23) \quad \Theta_1 = \tan^{-1}\omega\tau_1 \quad [\text{radians}],$$

$$(24) \quad \Theta_2 = \tan^{-1}\omega\tau_2 \quad [\text{radians}],$$

$$(25) \quad \Theta_3 = \tan^{-1}\omega\tau_3 \quad [\text{radians}],$$

and

$$(26) \quad \Theta_4 = \tan^{-1}\omega\gamma \quad [\text{radians}].$$

The phase response of the above expression is given by

$$(27) \quad \phi_H(\omega) = \psi_{\tan} - \Theta_L, \quad [\text{radians}],$$

where

$$(28) \quad \Theta_L = \Theta_2 + \Theta_3 - \Theta_1 \quad [\text{radians}],$$

$$(29) \quad \psi_{\tan} = \tan^{-1} \left(\frac{c}{d} \right) \quad [\text{radians}],$$

$$(30) \quad c = K_F \frac{\Omega_1}{R} \sin\phi,$$

$$(31) \quad d = 1 + K_F \frac{\Omega_1}{R} \cos\phi,$$

$$(32) \quad \phi = \Theta_L + \Theta_4 \quad [\text{radians}],$$

and

$$(33) \quad R = \Omega_2\Omega_3\Omega_4.$$

Examination of equations 30, 31, and 33 reveals that ψ_{\tan} can be in the IVth or Ist quadrant only, because of the possible values of c and d, i.e., ψ_{\tan} is initially a retardive angle which after reaching its maximum retardation swings through zero to a maximum positive turning point after which ψ_{\tan} ultimately approaches zero as $\omega \rightarrow \infty$. In order to avoid any misinterpretation in respect to the involved quadrants, the half angle formula should be used for ψ_{\tan} , i.e., equation 29 may be rewritten as

$$(34) \quad \psi_{\tan} = 2 \tan^{-1} \left(\frac{c}{[c^2 + d^2]^{1/2} + d} \right).$$

Evidently, if ψ_{\tan} in equation 34 becomes negative, this indicates retardation (IVth Quadrant) and if positive, progression occurs (Ist Quadrant). Usually, an S-shaped output signal as shown in figure 2a results when a time sequential signal is obtained by the scanning of optical information focused on a semiconductor target plate. This is due to the finite size of the scanning-beam diameter, its intensity distribution, and the spatial spread of the carriers, all of which are caused by the optical information. Thus, the assumption that the boundaries of the signal from its point of initiation could be identified in figure 1b will not hold. Figure 2b again shows the signal obtained by modifying the signal of

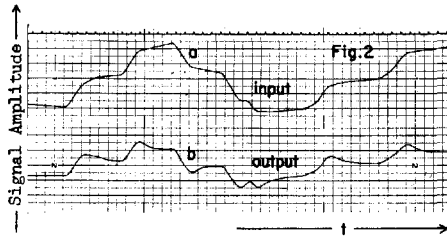


FIGURE 2. Time sequential signal, (a) obtained by slow scanning of image transducer; (b) showing effect of third order network on S-type distortion; each time marker represents 10 milli seconds.

figure 2a by a network represented by equation 1. The design data, mathematical relations, etc., needed for the construction of networks as represented by equations 1 and 2 are discussed.

THE ELECTRICAL ANALOG

A network with a transfer function as expressed by equations 1, 2, and 14 may be built as a closed-loop system (fig. 3) or as an open-loop system (fig. 4), using

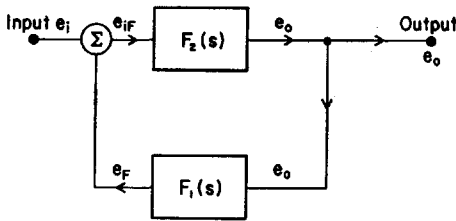


FIGURE 3. (Left) Black box diagram of closed loop system.

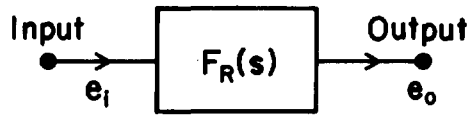


FIGURE 4. (Right) Black box diagram of open loop system.

operational amplifiers. For the closed-loop system of figure 3, equation 1 must be rewritten as

$$(35) \quad F_{RC}(s) = \frac{e_o}{e_i} = \frac{F_2(s)}{1 + F_1(s)F_2(s)},$$

where

$$(36) \quad F_2(s) = \frac{(1 + s\tau_1)}{(1 + s\tau_2)(1 + s\tau_3)},$$

and

$$(37) \quad F_1(s) = \frac{K_F}{(1 + s\gamma)}.$$

Then, the forward section,

$$(38) \quad F_2 = \frac{e_o}{e_{iF}} = \frac{(1 + s\tau_1)}{(1 + s\tau_2)(1 + s\tau_3)},$$

of the closed-loop system may be rewritten as

$$(39) \quad e_o = \frac{e_{iF}}{s^2} \frac{1}{\tau_2 \tau_3} + \frac{e_{iF}}{s} \frac{\tau_1}{\tau_2 \tau_3} + \frac{e_o}{s^2} \frac{1}{\tau_2 \tau_3} - \frac{e_o}{s} \frac{(\tau_2 + \tau_3)}{\tau_2 \tau_3}$$

shown in its analog form by figure 5. The feedback section of the closed-loop system

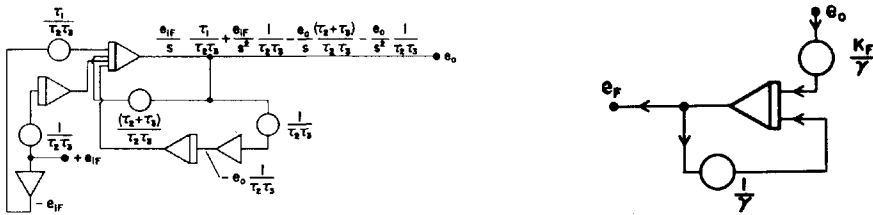


FIGURE 5. (Left) Analog diagram of forward section of closed loop system.
 FIGURE 6. (Right) Analog diagram of feedback section of closed loop system.

$$(40) \quad F_1 = \frac{e_F}{e_o} = \frac{K_F}{(1 + s\gamma)}$$

may be rewritten as

$$(41) \quad e_F = \frac{K_F e_o - e_F}{\gamma s}$$

shown in its analog form by figure 6. Figure 7 then shows the systems depicted by figures 5 and 6 combined into a closed-loop system.

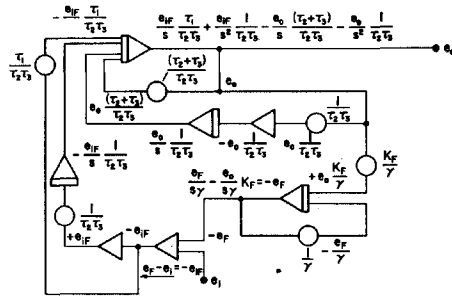


FIGURE 7. Diagram of arrangement of operational amplifiers of closed loop system.

Equation 1 may be rewritten for an open-loop transfer set-up (fig. 4) as

$$(42) \quad e_o = \frac{1}{\beta} \left\{ \mu e_i s^{-1} + \nu e_i s^{-2} + e_i s^{-3} \right\} - K_F \frac{1}{\beta} \left\{ \tau_1 e_o s^{-2} + e_o s^{-3} \right\} - \frac{1}{\beta} \left\{ \xi e_o s^{-1} + \gamma e_o s^{-2} + e_o s^{-3} \right\}$$

where

$$(43) \quad \mu = \tau_1 \gamma \quad [\text{sec}^2],$$

$$(44) \quad \nu = \tau_1 + \gamma \quad [\text{sec}],$$

$$(45) \quad \beta = \alpha \gamma \quad [\text{sec}^3],$$

$$(46) \quad \alpha = \tau_2 \tau_3 \quad [\text{sec}^2],$$

$$(47) \quad \xi + \alpha + \delta + \epsilon \quad [\text{sec}^2],$$

$$(48) \quad \delta = \gamma \tau_2 \quad [\text{sec}^2],$$

$$(49) \quad \epsilon = \gamma \tau_3 \quad [\text{sec}^2],$$

$$(50) \quad \Upsilon = \tau_2 + \tau_3 + \gamma \quad [\text{sec}^2],$$

or more conveniently as

$$(51) \quad e_o \left\{ \mu^\dagger e_i s^{-1} + \nu^\dagger e_i s^{-2} + \frac{e_i}{\beta} s^{-3} \right\} - K_F \left\{ \tau_1^\dagger e_o s^{-2} + \frac{e_o}{\beta} s^{-3} \right\} - \left\{ \xi^\dagger e_o s^{-1} + \Upsilon^\dagger e_o s^{-2} + \frac{e_o}{\beta} s^{-3} \right\},$$

$$(52) \quad \mu^\dagger = \mu / \beta \quad [\text{sec}^{-1}],$$

$$(53) \quad \nu^\dagger = \nu / \beta \quad [\text{sec}^{-2}],$$

$$(54) \quad \tau_1^\dagger = \tau_1 / \beta \quad [\text{sec}^{-2}],$$

$$(55) \quad \xi^\dagger = \xi / \beta \quad [\text{sec}^{-1}],$$

$$(56) \quad \Upsilon^\dagger = \Upsilon / \beta \quad [\text{sec}^{-2}].$$

Figure 8 shows the analog computer arrangement for the above open loop transfer functions of equation 51.

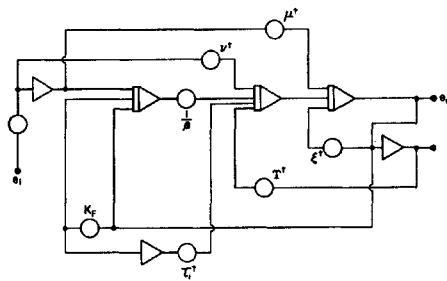


FIGURE 8. Diagram of arrangement of operational amplifiers of open loop system.

A TYPICAL EXAMPLE

The electronic-analog-computer arrangement and the processing for a slow-scan narrow-bandwidth signal is shown in the following typical example.

The system design parameters were chosen to be $\gamma = 0.02$ sec., $\tau_1 = 1/12.6$ sec., $\tau_2 = 1/333$ sec., $\tau_3 = 1/50.4$ sec. and $K_F = 0.25$. Figure 1 was obtained with the

above design parameters in an open loop arrangement. Figures 2 and 9 show the behavior of the system to a variable input. The behavior of the system with a variable input is shown by figures 2 and 9. The signal in figure 9 undergoes a smoothing effect for fast irregularities, but the edge steepening of the information portion of the signal is still accomplished. The frequency- and phase responses

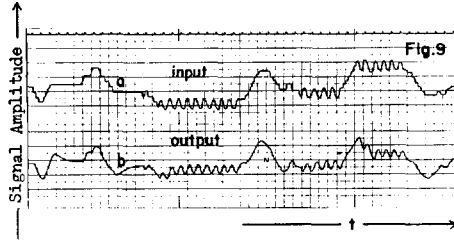


FIGURE 9. Smoothing effect of third-order system on time sequential signal.

of the typical arrangement, with γ as a parameter, are shown in figures 10 and 11. Figure 12 shows the Nyquist diagram of the transfer function in the frequency

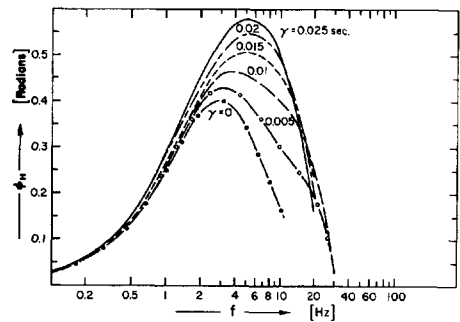
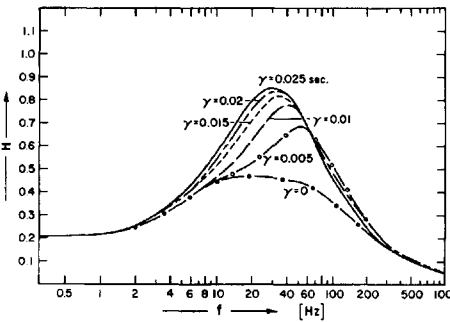


FIGURE 10. (Left) Frequency response of typical third-order system used as example for several values of the parameter γ .

FIGURE 11. (Right) Phase response of typical third-order system used as example for several values of the parameter γ .

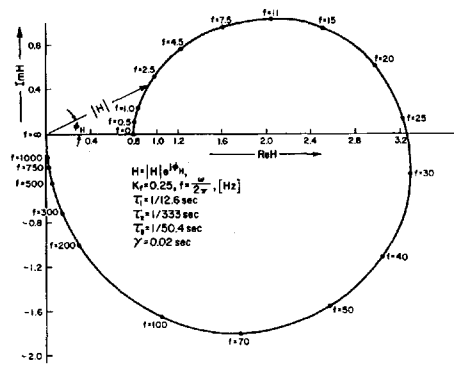
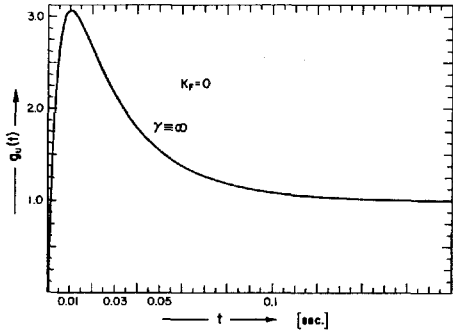
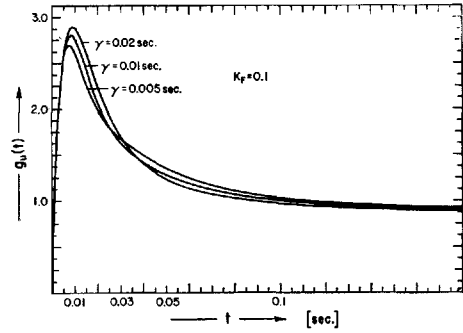


FIGURE 12. Nyquist diagram of transfer function of typical third-order system used as example.

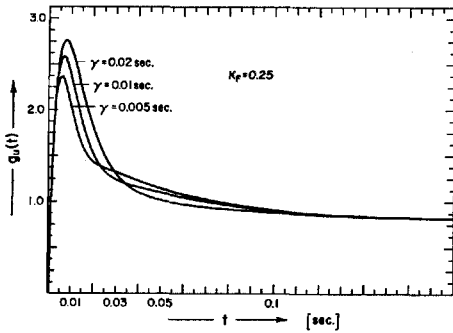
domain using the design parameters of the typical example. Figures 13a through 13e show the effects of varying the system parameters K_F and γ when applying a unit input step. These were obtained from the analytical expression in the time



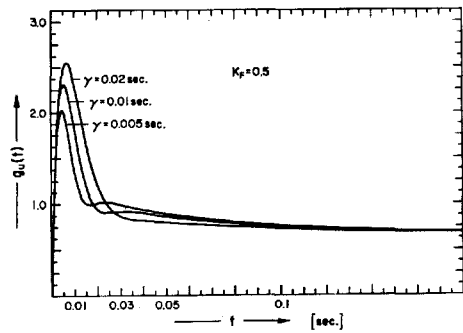
(13a)



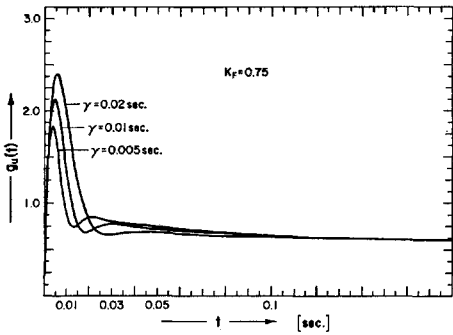
(13b)



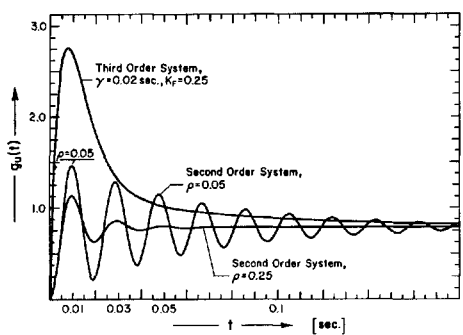
(13c)



(13d)



(13e)



(14)

FIGURE 13(a-e). Effect of variation of system parameters.

FIGURE 14. (Lower Right) Comparison of second- and third-order system time domain responses.

domain. Figure 14 compares the response to a unit step input in the time domain with that of a conventional second order system. The latter has a transfer function in the time domain given by the well-known equation (Ayre, 1961)

$$(57) \quad h_{2u}(t) = \rho\omega_o(1 - \rho^2)^{-1/2}e^{-\rho\omega_o t} \sin[(1 - \rho^2)^{1/2}\omega_o t] \quad [\text{sec}^{-1}],$$

which yields for a unit step input the relation

$$(58) \quad g_{2u}(t) = 1 - e^{-\rho\omega_0 t} \{ \cos[(1-\rho^2)^{1/2}\omega_0 t] + \rho(1-\rho^2)^{-1/2} \sin[(1-\rho^2)^{1/2}\omega_0 t] \},$$

where ρ is the ratio of the system damping constant to the critical damping, and ω_0 in radians sec^{-1} is the natural circular frequency of the undamped system. The time at which the first maximum occurs, found by differentiation of the above equation, is

$$(59) \quad t_{\max,1} = (1-\rho^2)^{-1/2} \omega_0^{-1} \quad [\text{sec}],$$

which gives for the natural frequency f_0 of the undamped system

$$(60) \quad f_0 = \omega_0 / 2\pi = 0.5(1-\rho^2)^{-1/2} t_{\max,1}^{-1} \quad [\text{Hz}].$$

The value of the relative amplitude of the first maximum, $g_{\mu, \max}$ is then given for this second order system by

$$(61) \quad g_{2u, \max} = 1 + e^{-\pi\rho(1-\rho^2)^{-1/2}}.$$

It should be noted that equation 61 yields a value which is always less than 2 and that the ideal value of 2 is approached only for $\rho \rightarrow 0$, a condition unrealizable in any practical situation. Figure 14 applies for a second-order system, the values $\rho=0.05$ and $\rho=0.25$ were selected and the value of ω_0 was chosen in such a way as to make the peak values of the relative amplitudes occur at nearly the same time. Figures 15 and 16 compare the frequency and phase responses of the

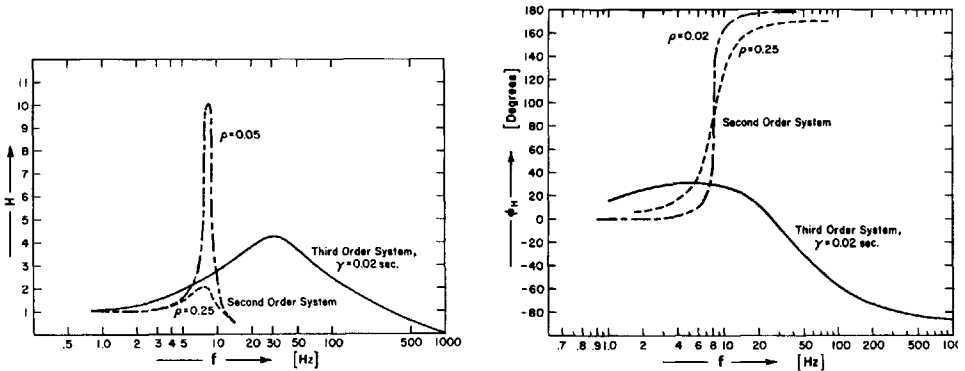


FIGURE 15. (Left) Comparison of second and third order system frequency domain responses.
 FIGURE 16. (Right) Comparison of second and third order system phase response.

typical example ($K_F=0.25, \gamma=0.02$) with those of a second order system. Figure 17 shows the systems behavior when the input signal (fig. 17a) is mixed with white noise. Figure 17b shows the output signal, which is edge steepened. However, a large portion of the random noise of the input signal is removed due to the

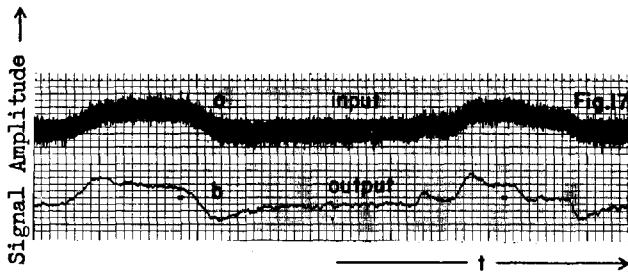


FIGURE 17(a & b). Behaviour of typical third-order system to white noise.

bandwidth limiting action of the arrangement. The values of the system parameters to be used evidently depend on the involved frequency range of the signal to be modified as well as on the form of the deterioration existing in the signal. Naturally, the upper cut off frequency of the operational amplifiers used must be sufficiently high to transmit all of the involved frequencies. The authors trust that the foregoing information will give design engineers sufficient basic data for determining appropriate networks applicable to any other situations.

ACKNOWLEDGMENTS

This research was performed under Projects 7885 and 7081 of the Aerospace Research Laboratories. The United States Patent 3,792,363 entitled "Controlable Edge Sharpening System for Time Sequential Signals" covering the subject matter of this paper was issued on Febr. 12, 74 to the United States of America as represented by the Secretary of the Air Force, Wash. D.C., with the authors of this paper as the inventors. We wish to express our sincere gratitude to Prof. Dr. Herman R. Weed, Director of Bio-Electrical Engineering Research at The Ohio State University, Columbus, Ohio, U.S.A. for encouragement, constructive criticism, and review of this paper. Appreciation is also given to Mr. Beecher W. Vaughn, 4950/VNA, for programming and operating the Comcor 5000 Analog Computer in connection with a Sigma 7, using a Comcor 5100 Intracom for analog to digital conversion and vice versa as a hybrid combination, in order to obtain the analog traces; to Mr. James Caslin, ARL/LB, for programming and operating the IBM 1620 Digital Computer and obtaining graphical representations of the time-response data on the Hewlett-Packard (9100A) programmable desk calculator; and to Mr. Joseph L. Dowdell, 4950th test wing (technical)/FTCC for programming the IBM 7094/7044 direct-coupled system in order to obtain response data in the frequency domain. Further, it is a pleasure to acknowledge the assistance of Mr. Roy R. Hayslett in the realization of this paper.

LITERATURE CITED

- Ayre, Robert S.** Transient response to step and pulse function, Chap. 8, p. 8-1 to 8-54. In Harris, Cyril M., and Charles E. Crede, Eds., Shock and Vibration Handbook, Vol. 1. McGraw-Hill, New York, 760 p.
- Creed, R. S., D. Denny-Brown, J. C. Eedes, E. G. T. Liddell, C. S. Sherrington.** 1932. Reflex activity of the spinal cord. Clarendon Press, New York, 179 p.
- Jacobson, L. S., and R. S. Ayre.** 1958. Engineering vibrations. McGraw-Hill Book Co., Inc., New York, 564 p.
- Lippold, O. C. J., J. G. Nicholls, and J. W. T. Redfearn.** 1960. Electrical and mechanical factors in the adaptation of a mammalian muscle spindle. *J. Physiol.* 153: 209-217.

Statistical Thinking: A Structural Approach. *John L. Phillips, Jr.* W. H. Freeman and Co., San Francisco. 1973. xv+124 p. Clothbound \$5.95. Paperbound \$2.50.

This small book is written for beginners in statistics. Students in fields such as education and the social sciences who have little mathematical knowledge but can do arithmetic are its intended readers. The author emphasizes his awareness that such students often have difficulties in learning mathematical statistics. His aim is to help these students to do mathematical statistics by helping them to understand the statistical concepts that lie behind it. Professor Phillips, a psychologist, has written this book to precede or supplement an introductory statistics course.

Numerous worked-out examples in the book are taken from education, psychology, and the social sciences. The first few chapters discuss frequency distributions, measures of central tendency, variability, and relationship. These beginning chapters are clearly written, but contain a few unproved mathematical relations. In the later chapters only sketchy presentations are found of such important topics as confidence levels, significance of a difference between two sample means using the t-test, and testing of hypotheses using the chi square test.

The book's aims to clarify statistical concepts are only partially fulfilled for the intended readership. Such students will have to look elsewhere to understand clearly many of the statistical concepts and tests briefly discussed in the second half of this book.

LAWRENCE A. WELLER